Catalysis of $NiO–Al_2O_3$ aerogels for the CO_2-reforming of CH_4

Toshihiko Osaki *, Tatsuro Horiuchi, Toyohiko Sugiyama, Kenzi Suzuki and Toshiaki Mori

National Industrial Research Institute of Nagoya, Hirate-cho, Kita-ku, Nagoya 462, Japan

Received 25 February 1998; accepted 6 April 1998

Uniform and monolithic $NiO–Al_2O_3$ aerogels were prepared from cyclic nickel glycoxide, $(CH_2O)_2Ni$, and boehmite sol, AlOOH, and the catalyst performance of the aerogels for the CO_2-reforming of methane was investigated. The $NiO–Al_2O_3$ aerogels showed higher activity than impregnation NiO/Al_2O_3 catalysts, while the aerogels exhibited much less activity for coking than the impregnation catalysts. Less deactivation was also observed on the aerogel catalysts than on the impregnation catalysts in the continuous-flow reaction. The Ni was uniformly incorporated throughout alumina where both the metal and the support exist in the aerogel form, i.e., Ni–O–Al bond was considered to be formed in the aerogels. As a result, fine Ni particles appeared after H_2 reduction throughout the alumina support with high dispersion, which brought about not only higher activity but also much less activity for coking on the aerogels. Retardation of catalyst deactivation was ascribed to the suppression of both coking and sintering of Ni particles on the aerogels.

Keywords: CO_2-reforming of CH_4, aerogel, $Ni–Al_2O_3$, carbon deposition, small ensemble

1. Introduction

It is of great interest to investigate the performance of aerogels as catalysts or catalyst supports. An aerogel is usually prepared by gelation of sol in a solvent followed by the removal of solvent under supercritical conditions. Generally, an aerogel has large surface area, low bulk density and large pore volume. A conventional technique to prepare a catalyst using the aerogel as a catalyst support involves impregnation of the aerogel in a desired metal salt solution, followed by evaporation of solvent and subsequent calcination. Unlike a conventional catalyst preparation, a cogel is prepared by employing two or more metal alkoxides as starting materials. A structure of M–O–M′ (M, M′ = metal) is constructed in the gel, and thereby a metal oxide is highly dispersed throughout the support after calcination. As for alumina aerogel-supported nickel oxide, a cogel was prepared by hydrolyzing and precipitating a solution of aluminium sec-butoxide in the presence of dissolved nickel acetate with vigorous stirring [1–8]. However, because the gelation of aluminium hydroxide occurs very rapidly, it is not easy to prepare a uniform cogel between aluminium and nickel. And it is also difficult to prepare a monolithic alumina-supported nickel oxide aerogel, because vigorous stirring of the alkoxides is required on mixing and hydrolyzing.

We developed a new method for preparing a uniform and monolithic nickel–alumina aerogel from cyclic nickel glycoxide, $(CH_2O)_2Ni$, and boehmite sol, AlOOH [9]. After the addition of cyclic nickel glycoxide to a transparent boehmite sol, urea was added to the mixed sol for gelation. The urea added was gradually decomposed in the solvent to give NH_4^+ ion, by which pH of the mixed sol increased gradually, while ζ-potential of the sol gradually decreased [10]. This resulted in gradual polymerization of the reactants to form a uniform Al–O–Ni chain throughout the aerogel.

We attempted to investigate the catalysis of the $NiO–Al_2O_3$ aerogels for the CO_2-reforming of CH_4:

$$CH_4 + CO_2 \rightleftharpoons 2CO + 2H_2 \quad \Delta G = 247\ \mathrm{kJ\,mol^{-1}} \qquad (1)$$

Since the CO_2-reforming of methane is an endothermic reaction with $\Delta G = 247\ \mathrm{kJ\,mol^{-1}}$, the reaction should be carried out at temperature above 1073 K. The aerogel catalysts might show high performance for the reaction because high surface area is maintained at elevated temperature. It is also expected that fine Ni particles on the aerogels would inhibit the carbon deposition since a large ensemble of nickel atoms is necessary for the nucleation of carbon. Here, the catalysis of $NiO–Al_2O_3$ aerogels is studied by comparing to NiO/Al_2O_3 catalysts prepared by conventional impregnation. For the impregnation catalysts, a commercial γ-alumina and an aerogel γ-alumina prepared by the method described above were used as catalyst supports.

2. Experimental

2.1. Preparation of $NiO–Al_2O_3$ aerogels

Detailed procedures for preparing $NiO–Al_2O_3$ aerogels and thermal analysis of the aerogels were described in a previous paper [9]. Here, we give a brief outline for the preparation. Aluminium triisopropoxide (20.4 g, 0.1 mol) was hydrolyzed with 80 ml of hot water in a flask and the resultant mixture was kept with vigorous stirring at 353 K for 1 h. To the cloudy sol, 0.01 mol of nitric acid was added for peptization and the sol was refluxed with stirring at 368 K for 1 h to obtain a clear sol. An appropriate

* To whom correspondence should be addressed.

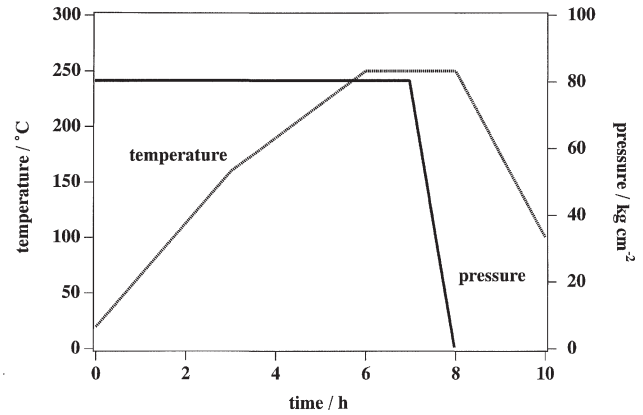

Figure 1. Temperature and pressure schedule for supercritical drying with ethanol.

amount (1.29 and 2.57 g for 5 and 10 wt% Ni–Al_2O_3 aerogels, respectively) of $Ni(NO_3)_2 \cdot 6H_2O$ (Wako Pure Chemical Industries, 98.0%) was dissolved in 2.58 ml of ethylene glycol and the solution was kept at 353 K for 30 min with stirring to obtain $(CH_2O)_2Ni$. The Ni chelate solution was then added to the clear boehmite sol and the resultant mixture was refluxed at 368 K for 1 h with vigorous stirring.

For gelation, urea (0.5 g) was added to the sol at 368 K with stirring. The amount of urea was half the amount of nitric acid on a mole base. Then, the sol was poured into a warmed Teflon vessel (i.d. 1.85 cm, height 3.33 cm), and the sol was kept at 368 K in a thermostat. The vessel was sealed with a Teflon stopper to prevent solvent evaporation.

The monolithic cogel obtained was put in a stainless-steel mesh container and dipped into 100 ml ethanol for 3 days to replace water, ethylene glycol, nitric acid and urea dissolved in the solvent with ethanol. Fresh ethanol was supplied once a day for complete substitution by ethanol. After aging in ethanol, the cogel was dried in ethanol under supercritical conditions (64 kg cm^{-2}, 243 °C). The schedule for removal of ethanol supercritically is shown in figure 1. After the supercritical drying, the cogel was calcined at 773 K for 4 h.

2.2. Preparation of impregnation NiO/Al_2O_3

For comparison with the aerogels, 10 wt% NiO/Al_2O_3 was prepared by impregnation using a commercial γ-Al_2O_3 (GL-Science, Active Alumina; surface area ca. 112 m^2 g^{-1}) and an aerogel γ-Al_2O_3 (surface area ca. 259 m^2 g^{-1}, see table 1) prepared by the method described above. For simplifying the description, the commercial γ-Al_2O_3 is denoted hereafter as "comm-Al_2O_3", while the aerogel γ-alumina is denoted as "aero-Al_2O_3". For further information, NiO–Al_2O_3 (dash) indicates the aerogel prepared by the method described above, while NiO/Al_2O_3 (slash) indicates the impregnation catalyst using comm-Al_2O_3 and aero-Al_2O_3 as a catalyst support: 1.65 g of nickel nitrate was dissolved in ion-exchanged and distilled water (150 ml), and 3 g of comm-Al_2O_3 and aero-Al_2O_3 were impregnated in the nickel solution. The water was evaporated gradually on an oil bath, and the impregnated alumina was dried at 383 K for one night in an electric desiccator. After drying, the sample was calcined at 773 K for 4 h in air. Before catalytic reaction, the catalyst was reduced with hydrogen. The Ni loading on Al_2O_3 is 10 wt% for both Ni/comm-Al_2O_3 and Ni/aero-Al_2O_3.

Table 1
BET surface area.

Catalyst	Surface area (m^2 g^{-1})
AlOOH	253.2
5 wt% Ni–AlOOH	276.2
10 wt% Ni–AlOOH	280.7
Al_2O_3	259.3
5 wt% NiO–Al_2O_3	321.9
10 wt% NiO–Al_2O_3	305.7
10 wt% NiO/aero-Al_2O_3	181.5
10 wt% NiO/comm-Al_2O_3	66.8

2.3. Temperature-programmed reduction

Reduction of NiO to Ni was investigated by a temperature-programmed reduction (TPR) method: ca. 25 mg of NiO–Al_2O_3 and NiO/Al_2O_3 was packed in a quartz tube (i.d. 4 mm) and heated in H_2–Ar (5 : 95) carrier gas (30 ml min^{-1}) from room temperature to 1273 K at 5 K min^{-1} rate. The consumption of H_2, due to NiO+H_2 $\rightarrow$ Ni + H_2O, was monitored continuously by gas chromatography with a thermal conductivity detector (Shimadzu, GC-8A). The reduction of NiO to Ni was also investigated by TG: ca. 20 mg of NiO–Al_2O_3 and NiO/Al_2O_3 was put in a TG quartz cell and heated from room temperature to 1273 K at 5 K min^{-1} in H_2 carrier gas, and the reduction of NiO to Ni was monitored by weight loss.

2.4. Characterization of catalysts

Surface area of the aerogels was measured by an N_2-adsorption apparatus (Japan Bel, Belsorp 28 SP) using the BET method at liquid-nitrogen temperature.

Crystalline phases of the aerogels were identified using an X-ray powder diffractometer (Rigaku, Rad-1VC) with a Cu tube operated at 30 kV and 20 mA.

The hemispherical transmittance spectra of the aerogels in normal incidence were recorded with a UV-visible spectrophotometer (Jasco, V-570). The aerogel was sandwiched by thin glasses and the directional transmittance measurement was carried out. The absorbances were corrected by subtracting the base line absorbances of the thin glasses.

The amounts of CO and H_2 adsorbed on the catalysts were measured at room temperature by a conventional pulse-adsorption method. After the reduction with hydrogen (30 ml min^{-1}) at 1073 K for 3 h, 0.54 ml of CO and H_2 was pulsed onto the catalyst in helium and argon carrier gas (30 ml min^{-1}), respectively, at room temperature for several times. The amounts of CO and H_2 adsorbed on the catalyst were calculated on a per gram of catalyst basis.

2.5. Steady-state CH_4–CO_2 reaction

The CO_2-reforming of CH_4 was performed in a conventional fixed-bed flow reactor at atmospheric pressure. Prior to the reaction, ca. 30 mg of catalyst (NiO–Al_2O_3 and NiO/Al_2O_3) packed in a quartz tube (i.d. 4 mm) was reduced with hydrogen (30 ml min^{-1}) at 1073 K for 3 h. After purging hydrogen with helium (30 ml min^{-1}) at 1073 K for 30 min, an equimolar mixture of CH_4 and CO_2 (total flow rate 60 ml min^{-1}) was continuously admitted to the reactor at 1073 K for 24 h. The effluent gas was analyzed at 30 min intervals by gas chromatography (Shimadzu, GC-14A) with a thermal conductivity detector using helium as the carrier gas. Combined columns of squalane, molecular sieve 5A and Porapak Q were used as separation columns.

The CH_4–CO_2 reaction was also investigated under differential reactor conditions. After reducing the catalyst with hydrogen followed by purging with helium, an equimolar mixture of CH_4 and CO_2 (total flow rate 60 ml min^{-1}) was introduced to the catalyst. The reaction was investigated in the temperature range 773–973 K, so that the conversion of methane in CH_4–CO_2 reaction should be less than 10%. The effluent gas was analyzed by gas chromatography with a thermal conductivity detector using separation columns as described above. The reaction rate per active site of a catalyst was calculated by dividing the CH_4-conversion rate by the number of adsorbed hydrogen atoms.

2.6. Coking in CH_4–CO_2 reaction

Carbon deposition on a catalyst during CH_4–CO_2 reaction was investigated by TG. After reducing NiO–Al_2O_3 and NiO/Al_2O_3 in a TG quartz cell with hydrogen (40 ml min^{-1}) at 1073 K for 200 min followed by purging hydrogen with helium (40 ml min^{-1}) at 1073 K for 10 min, an equimolar mixture of CH_4 and CO_2 (total flow rate 40 ml min^{-1}) was flowed over the catalyst at 1073 K. An increase of catalyst weight due to coking was monitored continuously.

2.7. Coking by CH_4 and dissociation of CO_2

Coking by CH_4 in the absence of CO_2 was investigated by TG. After the reduction of NiO–Al_2O_3 and NiO/Al_2O_3 in a TG quartz cell with hydrogen (40 ml min^{-1}) at 1073 K for 200 min, passing helium (40 ml min^{-1}) over the catalyst at 1073 K for 10 min, followed by the admission of CH_4 at 40 ml min^{-1} flow rate at 1073 K. An increase of catalyst weight due to carbon deposition, $CH_4 \rightarrow C + 2H_2$, was monitored continuously.

The ability of the catalyst to dissociate CO_2 in the absence of CH_4 was examined by a conventional pulse technique in helium carrier gas. After reducing the catalyst in hydrogen (30 ml min^{-1}) at 1073 K for 3 h, CO_2 (0.54 ml) was pulsed onto the catalyst in helium carrier gas (30 ml min^{-1}) at 1073 K using a gas sampler. The amount of CO_2 dissociated was calculated from that of CO produced by the surface reaction, $CO_2 \rightarrow CO + O_{ads}$.

2.8. Dependence of reaction rate on partial pressures of CH_4 and CO_2

Reaction orders were determined from the dependence of reaction rate on partial pressures of both CH_4 and CO_2 at 873 K under differential reactor conditions. The CH_4–CO_2 reaction was carried out by varying the partial pressure of one reactant gas in the pressure range 0.26–0.74 atm while keeping the partial pressure of another gas at 0.26 atm. Helium was used as a balance for keeping the total flow rate at 54 ml min^{-1}. In order to satisfy the differential reactor conditions, the catalyst amount was adjusted. The reaction rate on a per active site of catalyst basis was calculated from CH_4 conversion using the adsorption number of hydrogen atoms.

3. Results

3.1. Preparation of NiO–Al_2O_3 aerogels

Figure 2 shows X-ray diffraction (XRD) patterns of the aerogels after supercritical drying. The XRD patterns indicate that the aerogels have a γ-AlOOH structure. Ni-containing phases were not detected by XRD for 5 and 10 wt% Ni–AlOOH aerogels.

Figure 3 shows XRD patterns of the aerogels after calcination at 773 K for 4 h. For comparison, those of NiO/aero-Al_2O_3 and NiO/comm-Al_2O_3 prepared by impregnation are also shown. All the aerogels showed γ-Al_2O_3 diffraction peaks, indicating that the structure was changed from γ-AlOOH to γ-Al_2O_3 after the calcination. The XRD peaks of γ-Al_2O_3 are broad because of intrinsic disorder in the structure. Diffraction peaks of NiO were not identified for 5 and 10 wt% NiO–Al_2O_3 in contrast to the case for NiO/comm-Al_2O_3. As also for NiO/aero-Al_2O_3, NiO diffraction peaks were not observed.

UV-visible spectra of Ni–AlOOH and NiO–Al_2O_3 aerogels are shown in figure 4. Transparent aerogels were obtained for pure γ-AlOOH and γ-Al_2O_3, the spectra of which had no absorption peak in the visible range. Absorption peaks at 384 and 646 nm were observed for olive green Ni–AlOOH aerogels. Although the spectrum of $(CH_2O)_2Ni$ was not measured, nickel might be incorporated in the γ-AlOOH aerogel as $(CH_2O)_2Ni$. Absorption peaks at 366 and 600 nm were observed for blue green NiO–Al_2O_3 aerogels, indicating a blue shift in the absorption maximum by the calcination. The spectra of NiO–Al_2O_3 aerogels did not coincide with that of NiO having absorption peaks at 465 and 709 nm, suggesting that Ni atoms are incorporated throughout γ-Al_2O_3 aerogel by constructing Ni–O–Al bonding.

Table 1 shows BET surface areas of Ni–AlOOH and NiO–Al_2O_3 aerogels. The surface areas of NiO/aero-Al_2O_3

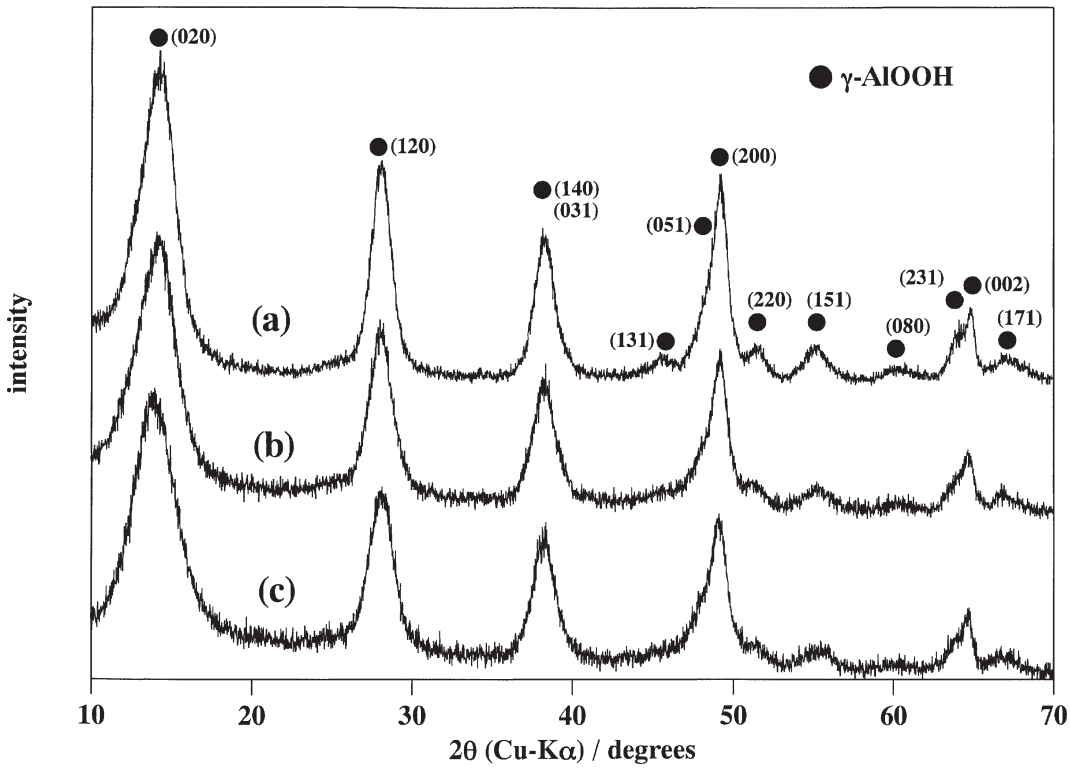

Figure 2. XRD patterns for aerogels after supercritical drying: (a) AlOOH, (b) 5 wt% Ni–AlOOH and (c) 10 wt% Ni–AlOOH.

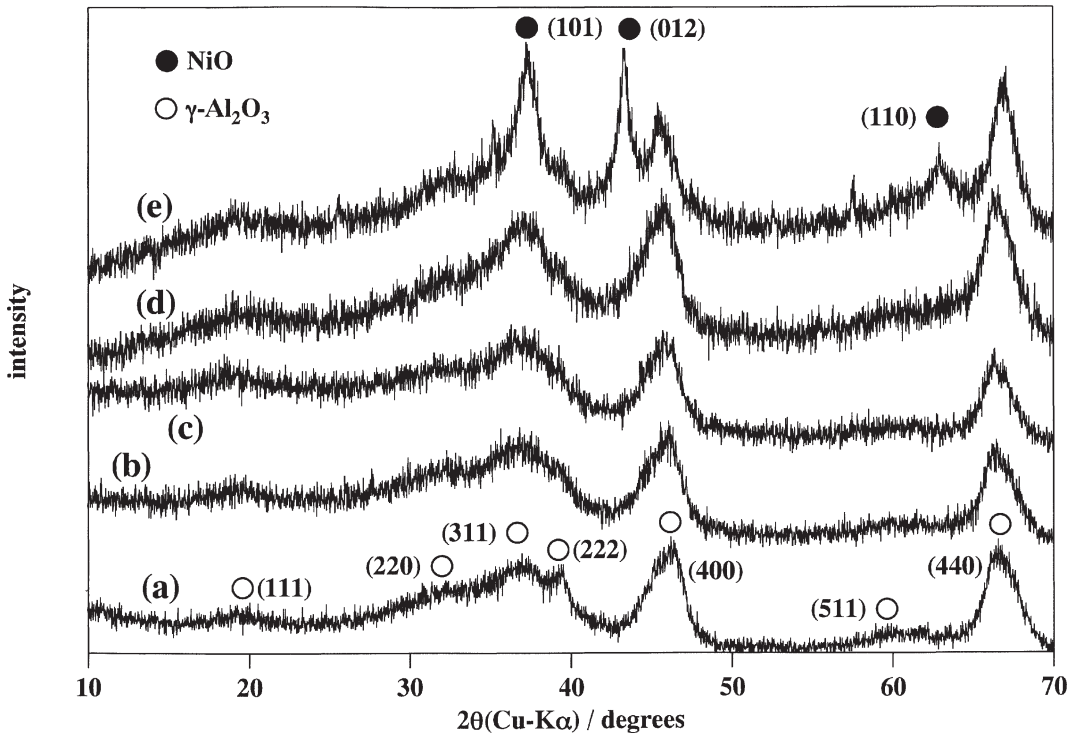

Figure 3. XRD patterns for aerogels and impregnation catalysts after calcination at 773 K for 4 h: (a) Al_2O_3 aerogel, (b) 5 wt% NiO–Al_2O_3 aerogel, (c) 10 wt% NiO–Al_2O_3 aerogel, (d) 10 wt% NiO/aero-Al_2O_3 and (e) 10 wt% NiO/comm-Al_2O_3.

and NiO/comm-Al_2O_3 are also shown for comparison. The surface area is larger for Al_2O_3 aerogels than for AlOOH aerogels. The addition of Ni increases the surface area for both AlOOH and Al_2O_3 aerogels. When 10 wt% NiO/aero-Al_2O_3 is prepared by impregnation using the aero-Al_2O_3 (surface area 259.3 $m^2\,g^{-1}$), the surface area is reduced to 181.5 $m^2\,g^{-1}$, which is ca. 70% surface area as large as that of the initial aerogel.

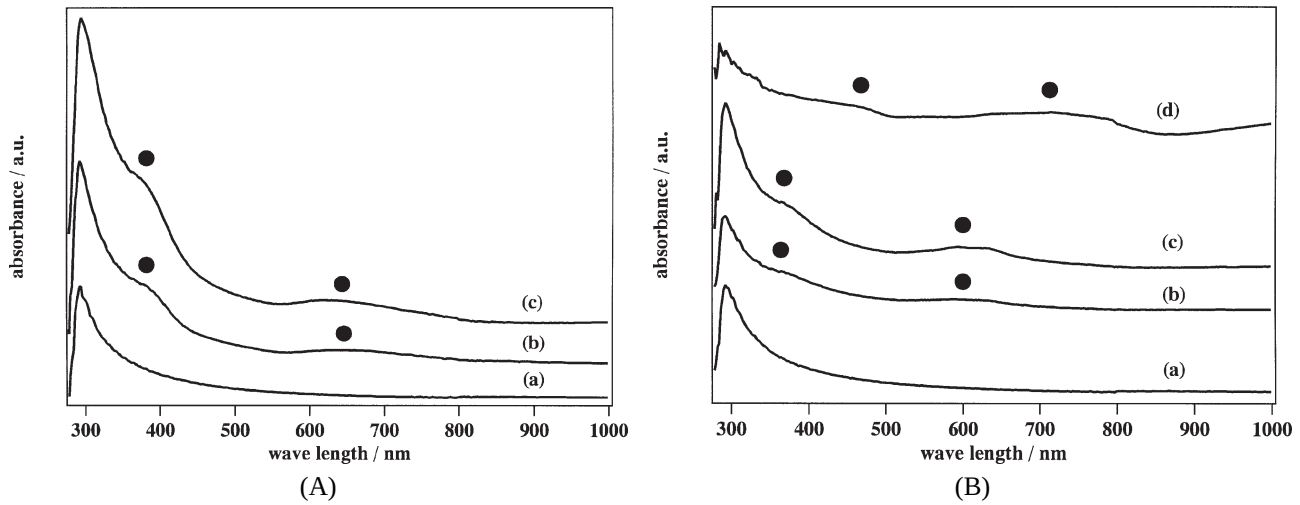

Figure 4. (A) UV-visible spectra of (a) AlOOH aerogel, (b) 5 wt% Ni–AlOOH aerogel and (c) 10 wt% Ni–AlOOH aerogel. (B) UV-visible spectra of (a) Al_2O_3 aerogel, (b) 5 wt% NiO–Al_2O_3 aerogel, (c) 10 wt% NiO–Al_2O_3 aerogel and (d) NiO.

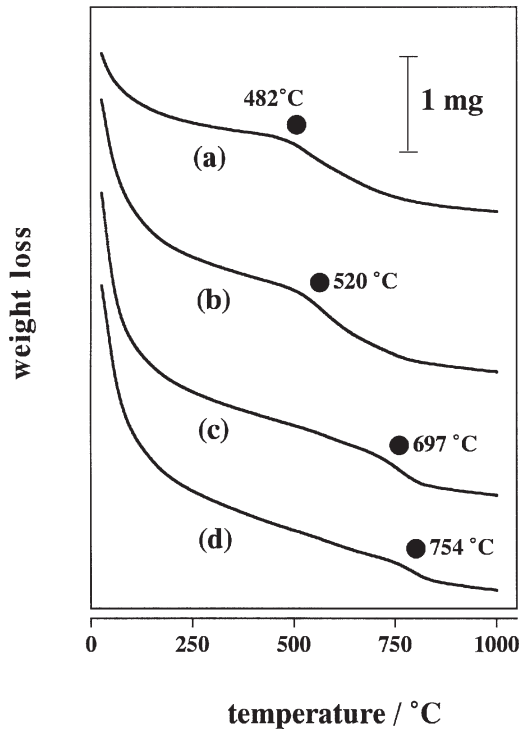

Figure 5. Thermogravimetry (TG) in H_2 for (a) 10 wt% NiO/comm-Al_2O_3 (20.0 mg), (b) 10 wt% NiO/aero-Al_2O_3 (20.1 mg), (c) 10 wt% NiO–Al_2O_3 aerogel (19.8 mg) and (d) 5 wt% NiO–Al_2O_3 aerogel (20.0 mg).

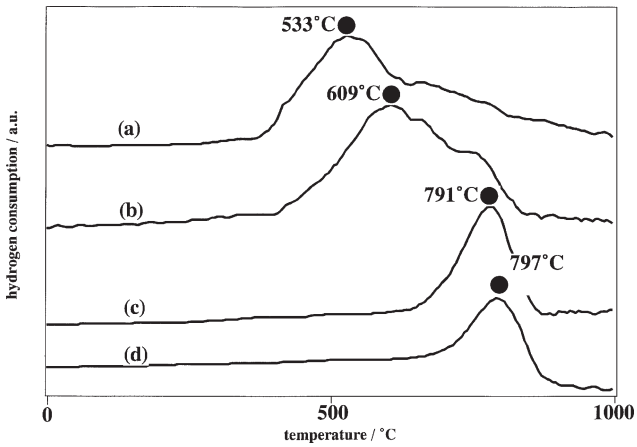

Figure 6. Temperature-programmed reduction (TPR) of (a) 10 wt% NiO/comm-Al_2O_3 (25.0 mg), (b) 10 wt% NiO/aero-Al_2O_3 (25.3 mg), (c) 10 wt% NiO–Al_2O_3 aerogel (25.2 mg) and (d) 5 wt% NiO–Al_2O_3 aerogel (25.7 mg).

3.2. Reduction of NiO

Results of TG for NiO–Al_2O_3 and NiO/Al_2O_3 in H_2 are depicted in figure 5. All the profiles are characterized by two kinds of weight loss, one is around 100 °C and the other is in the temperature range 480–750 °C. The former is ascribed to the liberation of free water adsorbed, while the latter can be ascribed to the reduction of NiO to Ni. TPR profiles also showed that H_2 consumption was observed in the temperature range 530–790 °C, as shown in figure 6, indicating the reduction of NiO to Ni. This temperature range corresponds to that for the latter weight loss in TG. The XRD analysis confirmed the appearance of Ni phase after the reduction, as shown in figure 7. No other nickel-containing phases were observed from XRD. The reduction occurred at higher temperature for aerogels than for impregnation catalysts. Between the aerogels, the reduction was observed at higher temperature for 5 wt% NiO–Al_2O_3 than for 10 wt% NiO–Al_2O_3. Between the impregnation catalysts, the reduction occurred at higher temperature for NiO/aero-Al_2O_3 than for NiO/comm-Al_2O_3. By comparison with the area of H_2 consumption in figure 6, relative extent of Ni reduction can be estimated. It seems that the extent of Ni reduction is lower for the aerogel catalysts than for the impregnation catalysts.

Table 2 summarizes CO adsorption, H_2 adsorption and Ni crystallite size. The amount of CO adsorption was about two times that of H_2 adsorption in spite of the possibility of nickel carbonyl formation. The two aerogels have the lowest CO/H ratio, which suggests that nickel carbonyl for-

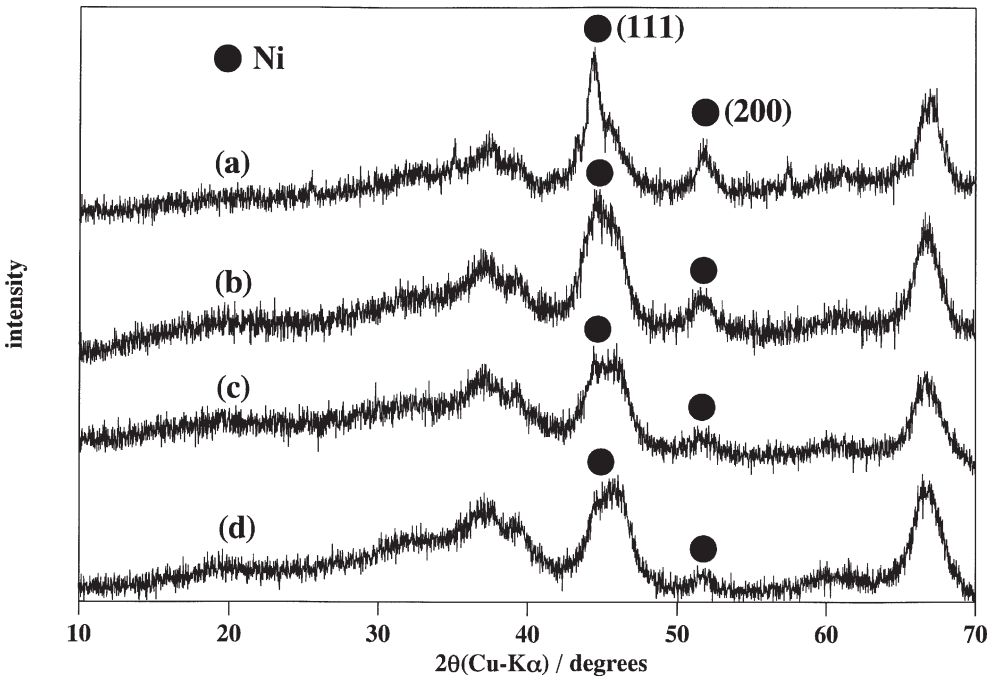

Figure 7. XRD patterns for aerogels and impregnation catalysts after reduction with hydrogen at 1073 K for 3 h: (a) 10 wt% Ni/comm-Al_2O_3, (b) 10 wt% Ni/aero-Al_2O_3, (c) 10 wt% Ni–Al_2O_3 aerogel and (d) 5 wt% Ni–Al_2O_3 aerogel.

Table 2
Gas adsorption and Ni crystallite size.

Catalyst	CO adsorption (μmol g^{-1})	H_2 adsorption (μmol g^{-1})	Ni crystallite size[a] (nm)
5 wt% Ni–Al_2O_3	16.31	9.08	2.88
10 wt% Ni–Al_2O_3	41.38	27.27	4.56
10 wt% NiO/aero-Al_2O_3	92.23	43.26	5.65
10 wt% NiO/comm-Al_2O_3	53.15	23.20	8.32

[a] Ni crystallite size was estimated by FWHM of Ni(200) using Scherrer's equation.

mation is more suppressed in these two samples. This inference means that Ni is more dispersed and interacting more strongly with the alumina support. Between the impregnation catalysts, the amount of H_2 adsorption was larger on Ni/aero-Al_2O_3 than on Ni/comm-Al_2O_3. This can be ascribed to smaller Ni particles on higher surface area Al_2O_3 support. Compared to the H_2 adsorption on Ni/aero-Al_2O_3, the amount was apparently smaller on 5 wt% Ni–Al_2O_3 and 10 wt% Ni–Al_2O_3. Taking into account the fact that the Ni crystallite size is smaller for 5 wt% Ni–Al_2O_3 and 10 wt% Ni–Al_2O_3 than for Ni/aero-Al_2O_3, Ni atoms in the aerogels are considered to be incorporated throughout Al_2O_3 by forming Ni–O–Al bonding, thereby some parts of Ni atoms appear on the surface after the reduction while other Ni atoms are still in the bonding.

3.3. Effect of time on stream

Figure 8 shows the effect of time on stream over 5 wt% Ni–Al_2O_3, Ni/aero-Al_2O_3 and Ni/comm-Al_2O_3 at 1073 K for 24 h. The methane conversion was compared on the

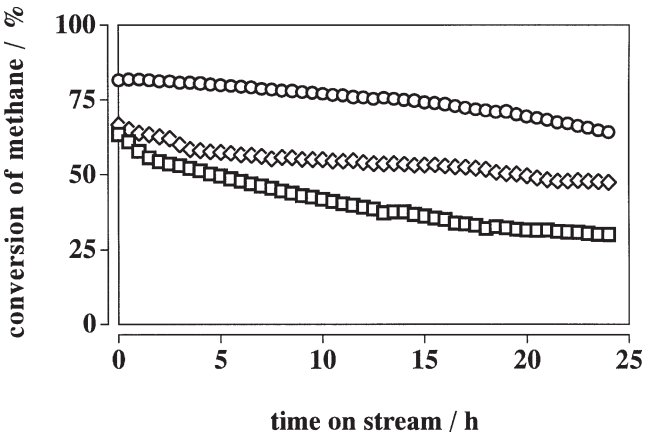

Figure 8. Catalytic activities with time on stream of CH_4–CO_2 (1 : 1, 60 ml min^{-1}) reaction at 1073 K on (○) 5 wt% Ni–Al_2O_3 aerogel (30.4 mg), (◇) 10 wt% Ni/aero-Al_2O_3 (31.1 mg) and (□) 10 wt% Ni/comm-Al_2O_3 (29.6 mg).

basis of catalyst weight. On Ni/comm-Al_2O_3, CH_4 conversion decreased rapidly with time on stream, from 63.4 to 30.0% for 24 h, as summarized in table 3. The ratio of methane conversion after 24 h, $C_{(24)}$, to the initial methane conversion, $C_{(0)}$, is 0.47. On Ni/aero-Al_2O_3, the deactivation was not so significant as that on Ni/comm-Al_2O_3. The $C_{(24)}/C_{(0)}$ for Ni/aero-Al_2O_3 is 0.71, which is higher than that for Ni/comm-Al_2O_3. The 5 wt% Ni–Al_2O_3 catalyst showed much higher activity than the impregnation catalysts in spite of half the amount of Ni loading. The deactivation was very little on the aerogel catalyst and the $C_{(24)}/C_{(0)}$ is 0.79. This was the largest ratio among the catalysts examined.

Table 3
Effect of time on stream.

Catalyst	Conv. of CH_4 (initial), $C_{(0)}$ (%)	Conv. of CH_4 (after 24 h), $C_{(24)}$ (%)	$C_{(24)}/C_{(0)}$	Ni crystallite size (after 24 h) (nm)
5 wt% Ni–Al_2O_3	81.6	64.2	0.79	3.93
10 wt% NiO/aero-Al_2O_3	66.7	47.5	0.71	9.43
10 wt% NiO/comm-Al_2O_3	63.4	30.0	0.47	20.2

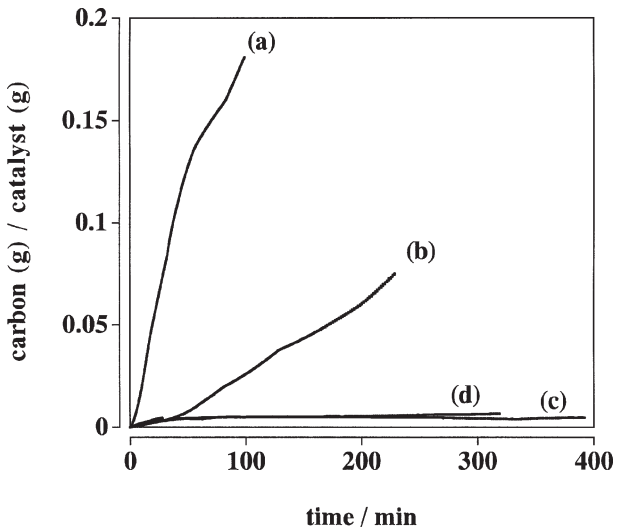

Figure 9. Carbon deposition in CH_4–CO_2 (1 : 1, 40 ml min^{-1}) reaction at 1073 K on (a) 10 wt% Ni/comm-Al_2O_3 (19.8 mg), (b) 10 wt% Ni/aero-Al_2O_3 (21.0 mg), (c) 10 wt% Ni–Al_2O_3 aerogel (11.5 mg) and (d) 5 wt% Ni–Al_2O_3 aerogel (12.7 mg).

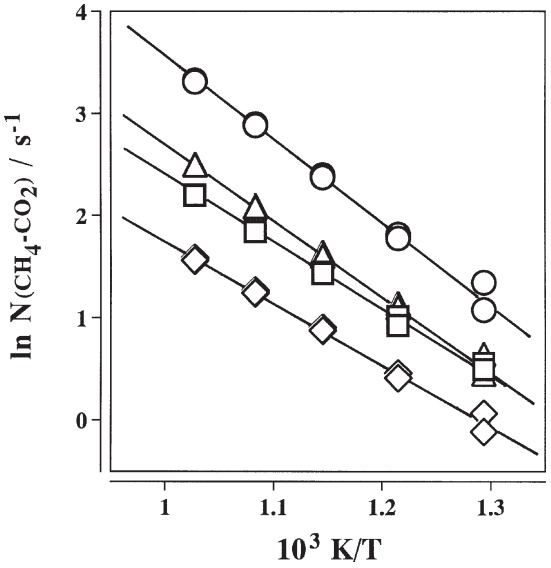

Figure 10. Arrhenius plots of reaction rates, $N_{(CH_4–CO_2)}$ (s^{-1}), for CH_4–CO_2 (1 : 1, 60 ml min^{-1}) reaction on (□) 10 wt% Ni/comm-Al_2O_3 (10.0 mg), (◇) 10 wt% Ni/aero-Al_2O_3 (10.3 mg), (△) 10 wt% Ni–Al_2O_3 aerogel (10.0 mg) and (○) 5 wt% Ni–Al_2O_3 aerogel (9.8 mg).

XRD analysis of the catalysts was carried out after the 24 h reaction. Table 3 shows Ni crystallite size after the reaction. For Ni/comm-Al_2O_3, Ni crystallite size was 20.2 nm, which was much larger than that of the initial one (8.32 nm, as summarized in table 2). For Ni/aero-Al_2O_3, Ni crystallite size was 9.43 nm, which was larger than that of the initial one (5.65 nm), but this change was not so marked as the case for Ni/comm-Al_2O_3. The Ni crystallite size for 5 wt% Ni–Al_2O_3 after the reaction was 3.93 nm. This was very close to the initial size (2.88 nm), suggesting that sintering of Ni particle was suppressed for the aerogel catalyst at elevated temperature. The suppression of sintering must be one of the causes for the retardation of catalyst deactivation.

Figure 9 shows carbon deposition during CH_4–CO_2 reaction at 1073 K. Among the catalysts, Ni/comm-Al_2O_3 showed the most significant coking during the reaction. The retardation of coking was observed on Ni/aero-Al_2O_3 compared to on Ni/comm-Al_2O_3. On 5 and 10 wt% Ni–Al_2O_3, very little coking was observed during the reaction in spite of their high activity for the reaction.

3.4. CH_4–CO_2 reaction under differential reactor conditions

The activity of the catalyst for the CO_2-reforming of methane was compared on the basis of specific activity. The rate per active site of a catalyst, $N_{(CH_4–CO_2)}$ (s^{-1}), is plotted in figure 10 as a function of reaction temperature. The specific activity was higher on the aerogel catalysts than on the impregnation catalysts, although the difference was small between 10 wt% Ni–Al_2O_3 and Ni/comm-Al_2O_3. Between the aerogel catalysts, the specific activity was higher on 5 wt% Ni–Al_2O_3 than on 10 wt% Ni–Al_2O_3, while between the impregnation catalysts, the activity was higher on Ni/comm-Al_2O_3 than on Ni/aero-Al_2O_3. The activation energy is summarized in table 4. The activation energy is higher for the aerogel catalysts than for the impregnation catalysts.

3.5. Coking by CH_4 and dissociation of CO_2

Coking by CH_4 in the absence of CO_2 was investigated by TG, and the results are shown in figure 11. The coking was observed on all the catalysts soon after the admission of methane. The coking still continued for Ni/comm-Al_2O_3 and Ni/aero-Al_2O_3, while no further coking was observed for both 5 and 10 wt% Ni–Al_2O_3. Between the impregnation catalysts, the coking was more enhanced on Ni/comm-Al_2O_3 than on Ni/aero-Al_2O_3. On Ni/comm-Al_2O_3, the coking occurred in a logarithmic fashion of time, while it was in an exponential fashion of time on Ni/aero-Al_2O_3.

Table 4
Activation energy, CO_2 dissociation rate and reaction order.

Catalyst	Activation energy (kJ mol^{-1})	N_{CO_2} [a] (s^{-1})	Reaction order	
			a (CH_4)	b (CO_2)
5 wt% Ni–Al_2O_3	64.1	1.85	−0.30	0.10
10 wt% Ni–Al_2O_3	61.5	1.01	−0.29	0.13
10 wt% NiO/aero-Al_2O_3	49.1	0.85	−0.34	0.074
10 wt% NiO/comm-Al_2O_3	51.7	1.15	−0.33	0.070

[a] Apparent rate at 1073 K, $N_{CO_2} = (F/W)(C/100)(1/S_H)$ (s^{-1}), where F = carrier flow rate (mol s^{-1}), W = catalyst weight (g), C = conversion of CO_2 at pulse number = 1 (%), and S_H = hydrogen atoms adsorption number per catalyst weight (mol g^{-1}).

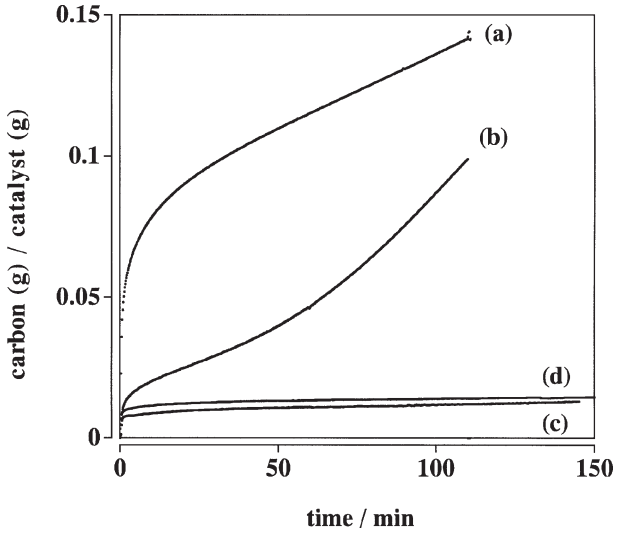

Figure 11. Activities for CH_4 dissociation in the absence of CO_2 at 1073 K on (a) 10 wt% Ni/comm-Al_2O_3 (21.7 mg), (b) 10 wt% Ni/aero-Al_2O_3 (18.8 mg), (c) 10 wt% Ni–Al_2O_3 aerogel (11.5 mg) and (d) 5 wt% Ni–Al_2O_3 aerogel (13.1 mg).

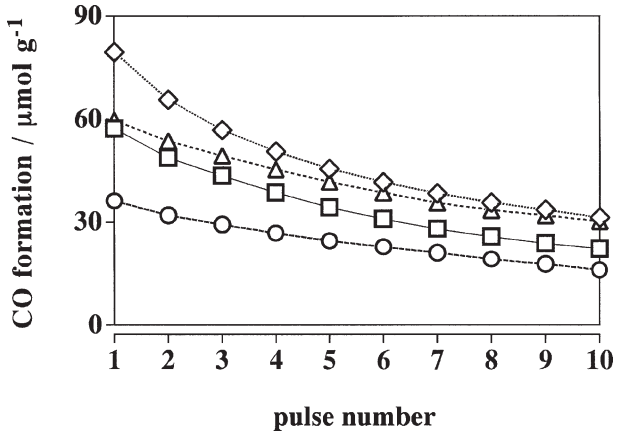

Figure 12. Activities for CO_2 dissociation in the absence of CH_4 at 1073 K on (□) 10 wt% Ni/comm-Al_2O_3 (57.3 mg), (◇) 10 wt% Ni/aero-Al_2O_3 (58.3 mg), (△) 10 wt% Ni–Al_2O_3 aerogel (32.0 mg) and (○) 5 wt% Ni–Al_2O_3 aerogel (35.1 mg).

The CO_2 dissociation in the absence of CH_4 was investigated by a pulse technique. The results are shown in figure 12. For all the catalysts, the amount of CO formed gradually decreased with pulse number, indicating that the active sites for $CO_2 \rightarrow CO + O_{ads}$ were gradually filled with adsorbed atomic oxygen, O_{ads}. It seems that ten pulses of CO_2 are not sufficient to cover completely the active sites with atomic oxygen. The apparent CO_2 dissociation rate per active site, N_{CO_2} (s^{-1}), is calculated, and the results are shown in table 4.

3.6. Dependence of reaction rate on CH_4 and CO_2 partial pressures

The dependence of reaction rate on partial pressures of both CH_4 and CO_2 is shown in figure 13. The reaction rate, ν, for CH_4–CO_2 is expressed as follows:

$$\nu = kP^{a}_{(CH_4)}P^{b}_{(CO_2)}, \quad (2)$$

where k is a rate constant, $P_{(CH_4)}$ and $P_{(CO_2)}$ are the partial pressures of CH_4 and CO_2, respectively, and a and b are the reaction orders with respect to partial pressures of CH_4 and CO_2, respectively. From the slopes of the straight lines for

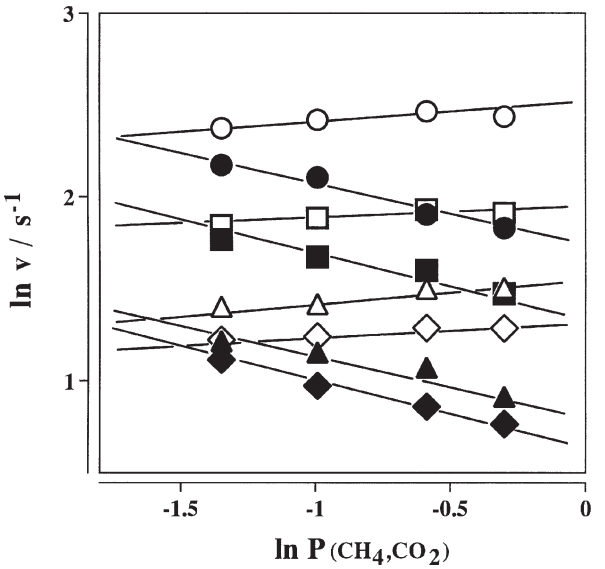

Figure 13. Dependence of reaction rate, v/s, on partial pressures of CH_4 and CO_2 at 873 K on (□, ■) 10 wt% Ni/comm-Al_2O_3 (7.0 mg), (◇, ◆) 10 wt% Ni/aero-Al_2O_3 (8.6 mg), (△, ▲) 10 wt% Ni–Al_2O_3 aerogel (6.7 mg) and (○, ●) 5 wt% Ni–Al_2O_3 aerogel (9.4 mg). Open symbols refer to rates with respect to partial pressure of CO_2, while closed symbols refer to rates with respect to partial pressure of CH_4.

$\ln \nu$ versus $\ln(P_{(CH_4)}, P_{(CO_2)})$, the reaction orders, a and b, can be calculated as shown in table 4. The reaction order with respect to partial pressure of CH_4 is negative, while that with respect to partial pressure of CO_2 is positive for all the catalysts. Compared to the impregnation catalysts, the reaction orders with respect to both CH_4 and CO_2 partial pressures are slightly larger for the aerogel catalysts, although the difference is very small.

4. Discussion

4.1. Preparation of uniform and monolithic NiO–Al_2O_3 aerogels

The combination of sol–gel technique with supercritical drying has been employed to synthesize highly distributed fine metal particles throughout an aerogel support. The cogel using metal alkoxides as starting materials is free from impurities. The hydrolysis of premixed metal alkoxides is one of the best ways for preparing fine metal particles on an aerogel support.

As for NiO–Al_2O_3 aerogels, the cogel was prepared by coprecipitation from an alcoholic solution of nickel acetate and aluminium sec-butoxide by the hydrolysis with a stoichiometric amount of water [1–8]. However, because hydrolysis of aluminium alkoxide and subsequent polymerization is rapid enough to give a precipitate of the gel soon after the contact with water, the solution must be stirred during mixing.

In contrast to the previous method, our method for preparing an Ni–Al cogel is novel in view of the following aspects: (1) an Ni–Al cogel is prepared from a uniformly mixed cosol of $(CH_2O)_2Ni$ and AlOOH by increasing the pH gradually; (2) since it takes some hours for polymerization of the cosol, a uniformly mixed cogel of Ni and Al can be obtained, thereby Ni–O–Al bonding is uniformly constructed throughout the aerogel after the calcination; (3) because it is not necessary for the cosol to be stirred during the gelation, the cosol can be poured into an appropriate vessel to make a monolithic cogel with a desired shape. Although precise investigations for gelation of the cosol have not been carried out, the gelation rate seems to be dependent not only on the amount of urea added for increasing the pH but also on the amount of ethylene glycol used for making cyclic nickel chelate. Further studies are necessary for the ambiguous discussion.

After the calcination of Ni–AlOOH aerogels at 773 K for 4 h, NiO peaks were not observed by XRD, as shown in figure 5. This suggests that the sol–gel technique ensures uniform distribution of Ni throughout Al_2O_3 by constructing Ni–O–Al bonding. The calcination of the boehmite aerogels caused not only a structure change to alumina but also an increase of surface area. Incorporation of Ni also increased the surface area for both AlOOH and Al_2O_3 aerogels. This might be because nickel chelate inhibits the crystallization of aluminium oxide when the cosol polymerizes to give the cogel.

After the reduction with hydrogen at 1073 K, the existence of Ni is first proved by XRD. TPR experiments indicate that the reduction of NiO in NiO–Al_2O_3 is more difficult than that in NiO/Al_2O_3, because NiO reduction occurred at higher temperature for the aerogels than for the impregnation catalysts. Taking into account the smaller H_2 adsorption number on the aerogels in spite of the smaller Ni crystallite size, some parts of NiO in the aerogels are reduced to Ni, in contrast to the case of the impregnation catalysts where most of NiO would be reduced to Ni. This is because NiO particles in the impregnation catalysts are attached on the surface of Al_2O_3 support, while Ni atoms in the aerogels are incorporated in the structure.

4.2. Catalysis for the CO_2-reforming of methane

A catalyst is often deactivated with time on stream due to sintering of active metal particles and/or to accumulation of carbonaceous deposit on active sites. Especially, for an endothermic reaction such as the CO_2-reforming of methane, since the reaction is usually carried out at elevated temperatures, a nickel catalyst is easily deactivated with time on stream due to both causes. To suppress the carbon deposition, addition of basic metal oxides such as K_2O and MgO to Ni is effective [11]. Using a basic metal oxide as a catalyst support is also an attractive way to retard the coking [12]. In any case, the reforming rate must be compromised with the coking rate to design a carbon-free Ni catalyst so that the coking rate should be more reduced than the reforming rate.

Carbon-free reforming reaction is successfully obtained on a partly sulfur-passivated Ni catalyst, called SPARG process [13,14]. On the sulfur-passivated catalyst, the coking rate is more reduced than the reforming rate. This is explained by assuming that a large ensemble of nickel atoms is necessary for the nucleation of carbon, whereas the reforming reaction proceeds on a small ensemble.

The catalyst performance of the aerogel is explicable in the same way. On the aerogel, very low coking occurred during the CH_4–CO_2 reaction while keeping a stable activity, and very low sintering of Ni was observed. The aerogel catalyst consists of only Ni and Al in contrast to the case of the alkali- or sulfur-promoted Ni on Al_2O_3 catalyst. The high performance of the aerogel catalyst for the CO_2-reforming of methane must, therefore, be due to the fine and uniform Ni particles distributing throughout alumina aerogel with high dispersion.

The effect of small ensembles seems to be observed for the aerogels: (1) the activation energy on the aerogel catalysts is higher than that on the impregnation catalysts; (2) between the aerogels, the activation energy is a little higher on 5 wt% Ni–Al_2O_3 than on 10 wt% Ni–Al_2O_3; (3) the reaction orders with respect to partial pressures of both CH_4 and CO_2 are slightly different between the aerogel and the impregnation catalyst. As shown in figure 11, the aerogels showed as high activity for the coking as the impregnation catalysts in the initial period of time, while

they did not show any activity after a constant amount of carbon was deposited on the active sites. It is reported for a supported Ni catalyst that carbon deposit is infinitely accumulated by constructing carbonaceous fibers, on the top of which Ni particles exist [15]. On the impregnation catalysts, the fibrous carbon must be accumulated between Ni particle and the alumina support. On the aerogels, on the other hand, it seems very difficult for the carbonaceous deposit to peel a fine Ni particle off the alumina aerogel support. This may be also evidence of the small ensembles on the aerogels.

To clarify the small ensembles on the aerogels, changing the Ni particle size at least in the range 1–25 nm would be informative. The particle size on the aerogels is easily varied by changing Ni concentration as reported for Ni–SiO_2 aerogel [16]. Therefore, an aerogel is very advantageous to control the particle size for suppressing the carbon nucleation.

5. Conclusions

The NiO–Al_2O_3 aerogel was prepared from cyclic nickel glycoxide and boehmite sol. The aerogel had surface area more than 300 $m^2\,g^{-1}$, while an impregnation NiO/aero-Al_2O_3 catalyst had ca. 70% surface area as large as that of the initial Al_2O_3 aerogel. The Ni in the aerogel was incorporated throughout Al_2O_3 support, where Ni–O–Al bonding was considered to be formed with high dispersion. The aerogel had high catalytic activity for the CO_2-reforming of methane. Carbon deposition and sintering of Ni were almost unobserved on the aerogel during the CH_4–CO_2 reaction, which was in contrast to the case on the impregnation catalysts. Since there was no additive such as basic metal oxide or sulfur to Ni, the high performance was primarily ascribed to the fine and uniform Ni particles distributing throughout the aerogel.

References

[1] S.J. Teichner, G.A. Nicolaon, M.A. Vicarini and G.E.E. Gardes, Adv. Colloid Interface Sci. 5 (1976) 245.
[2] G.E.E. Gardes, G.M. Pajonk and S.J. Teichner, J. Catal. 33 (1974) 145.
[3] M. Astier, A. Bertrand, D. Bianchi, A. Chenard, G.E.E. Gardes, G. Pajonk, M.B. Taghavi, S.J. Teichner and B.L. Villemin, Stud. Surf. Sci. Catal. 1 (1976) 315.
[4] S. Abouarnadasse, G.M. Pajonk, J.E. Germain and S.J. Teichner, Appl. Catal. 9 (1984) 119.
[5] S. Abouarnadasse, G.M. Pajonk, S.J. Teichner and J.E. Germain, Can. J. Chem. Eng. 62 (1984) 521.
[6] S. Abouarnadasse, G.M. Pajonk and S.J. Teichner, Appl. Catal. 16 (1985) 237.
[7] M. Rahman, R.J. Willey and S.J. Teichner, Appl. Catal. 36 (1988) 209.
[8] J.N. Armor, E.J. Carlson and P.M. Zambri, Appl. Catal. 19 (1985) 339.
[9] T. Osaki, T. Horiuchi, T. Sugiyama, K. Suzuki and T. Mori, J. Non-Cryst. Solids, in press.
[10] T. Horiuchi, T. Osaki, T. Sugiyama, H. Masuda, M. Horio, K. Suzuki, T. Mori and T. Sago, J. Chem. Soc. Faraday Trans. 90 (1994) 2573.
[11] T. Horiuchi, K. Sakuma, T. Fukui, Y. Kubo, T. Osaki and T. Mori, Appl. Catal. 144 (1996) 111.
[12] O. Yamazaki, T. Nozaki, K. Omata and K. Fujimoto, Chem. Lett. (1992) 1953.
[13] J.R. Rostrup-Nielsen, J. Catal. 85 (1984) 31.
[14] J.R. Rostrup-Nielsen, J. Catal. 144 (1993) 38.
[15] I. Alstrup, J. Catal. 109 (1988) 241.
[16] A. Ueno, H. Suzuki and Y. Kotera, J. Chem. Soc. Faraday Trans. 79 (1983) 127.